Effect of Slip Velocity on a Magnetic Fluid Based Squeeze Film in Rotating Transversely Rough Curved Porous Circular Plates

Mohmmadraiyan M. Munshi[1*]   A. R. Patel[2]   G. M. Deheri[3]

1.Department of Applied Science and Humanities, Alpha College of Engineering and Technology, Gujarat Technological University, Kalol, 382721, Gujarat, India

2.Department of Mathematics, Vishwakarma Government Engineering College, Gujarat Technological University, Ahmedabad, 382424, Gujarat, India

3.Department of Mathematics, Sardar Patel University, Vallabh Vidhyanagar, Anand, 388120, Gujarat, India

Abstract

This paper studies the effect of slip velocity on a magnetic fluid based squeeze film in rotating rough curved porous circular plates. The studied surfaces are assumed to be transversely rough. The surface of the upper curved plate is calculated using an exponential function and towards the lower curve plate along the surface administered by a secant function. The slip model created by Beavers-Joseph has been used to evaluate the impact of slip velocity. The roughness is designed using the stochastic method of Christensen and Tonder. The results of the related Reynolds type equation are used to determine the pressure distribution after which the final load carrying capacity is calculated. The results confirm the fact that the bearing system displays a better performance as opposed to the traditional fluid based bearing system. The roughness has a staunch impact on the bearing system. For ensuring a better performance, it is suggested that the slip parameter must be set at the minimum level.

Keywords: Circular plates, magnetic fluid, roughness, loads carrying capacity, slip velocity.

1. Introduction

Magnetic fluids have a lot of applications these days including the sealing of hard drives, x-ray tubes, rotating shafts and rods or as lubricants in various dampers and bearings. They are even being used as heat controllers present in electric motors. Some hi-fi speaker systems are now also using magnetic fluids. Ferro fluids are being used in a lot of scientific devices that are based on magnetic fluids. This includes sensors, accelerometers, pressure transducers, etc. They are also being used in actuating machines, electromechanical converters and energy converters, etc. Magnetic fluids have been found useful in biomedicine as well. Using alternating magnetic fields and heating magnetic fluid soaked tumours as a part of cancer treatment is also becoming popular.

Hays (1963) studied the normal approach of flat and curved rectangular plates that are divided using a thin film of lubricant, theoretically. Moore (1965) gave some fundamental equations including the impacts of inertia, variable viscosity, non-Newtonian fluids, surface tension, dynamic loading and surface roughness. Kuzma (1968) examined impacts of fluid inertia in squeeze film lubrication. Christensen & Tonder (1969a,b, 1970) designed two separate forms of Reynolds-type equation for two types of surface roughness using the stochastic theory and studied the functional impacts of surface roughness on the operational features of a plane pad, no side leakage slider bearing. Sparrow et al. (1972) studied the fluid flow method for a squeeze film having a porous wall. Wu (1972) worked on understanding the squeeze film performance between two separate rectangular plates when one of them had a porous facing and studied the impact of the porous facing on the squeeze film behaviour. Murti (1973) dealt with the squeeze film behaviour between two circular disks. Prakash & Vij (1973) studied the squeeze films between porous plates of various shapes. Gupta et al. (1982) analyzed the squeeze film performance between rotating annular plates theoretically for the situation when the curved upper plate with a uniform porous facing advanced normally towards the impermeable flat lower plate. Prakash & Tiwari (1983) suggested that the stochastic theory of hydrodynamic lubrication of rough surfaces assisted the study of impact of surface roughness on the reaction of a squeeze film between two circular plates when one of the plates had a porous facing. Prajapati (1992) embarked on the study of squeeze film behaviour present between rotating porous circular plates having a concentric circular pocket. Naduvinamani & Gurubasavaraj (2004) made use of the stochastic theory of hydrodynamic lubrication of rough surfaces to understand the impact of surface roughness on the squeeze film performance between a circular curved plate and a flat plate. Kumar & Rao (2015) worked with a generalized form of Reynolds equation for the two surfaces by hypothesizing the surface roughness of the bearing surfaces and acquired expressions for the according load capacity and squeezing time. Patel (1980) deliberated on the impacts of velocity slip on the nature of a squeeze film present between two circular disks in the situation where a uniform magnetic field was applied between them. Verma (1986) dealt with the squeeze film lubrication on a magnetic fluid between two surfaces approaching each other in the presence of an externally applied magnetic field which was placed oblique to the lower surface.

Shah & Bhat (2000) modified the impact of magnetic fluid lubrication on the work of the squeeze film that was created when an upper plate with a curved design and a porous facing advanced towards an impermeable and flat lower plate by understanding the rotation of the plates. Tripathi et al. (2002) studied the squeeze film behaviour

that took place between rotating annular plates theoretically when the upper plate with a curved design and a uniform porous facing advanced towards the impermeable and flat lower plate, by considering a magnetic fluid lubricant present with an external magnetic field oblique to the plates. Patel & Deheri (2002) studied the squeeze film action between two curved circular plates, when the upper plate moves towards the stationary curved lower plate. The lubricant used for the study was a magnetic fluid present with an external magnetic field placed oblique to the radial axis. Patel et al. (2017) investigated the action of a hydrodynamic journal bearing system based on ferrofluid with various shaft and bearing material combinations. A through research was carried out for the ideal combination of materials of ferrous and non-ferrous for shaft and bearing respectively, using a ferrofluid. Shimpi & Deheri (2012) analyzed the squeeze film behavior present between a rough porous circular plate with a curved shaped and another rough porous circular plate having a flat shape with the presence of a magnetic fluid lubricant. Shimpi & Deheri (2012) discussed on the squeeze film action between rotating transversely rough curved porous annular plates in the presence of a magnetic fluid lubricant while taking into consideration, the effect of elastic deformation. The study suggested that the deformation caused indeed impacted the load-carrying capacity in a negative way which got further declined because of porosity. This study concluded that negative impact of porosity, standard deviation and deformation can be neutralized to some extent using the positive impact of the magnetic fluid lubricant in the negatively skewed roughness situation by carefully selecting the ideal rotational inertia and the aspect ratio, especially for the appropriate ratio of curvature parameters.

Abhangi & Deheri (2012) examined the behaviour of a squeeze film based on magnetic fluid between curved transversely rough rotating circular plates when the upper plate placed along a surface determined by an exponential function advanced towards the curved lower plate on the surface according to a secant function. It was found that although the bearing was negatively impacted due to the transverse surface roughness, there was ample opportunity for obtaining a comparatively enhanced performance for negatively skewed roughness by carefully selecting the curvature parameters and the rotation ratio.

This paper aimed to study the impact of slip velocity on the configuration of (Abhangi & Deheri, 2012).

2. Analysis

The bearing which is displayed in Figure (1) (Abhangi & Deheri, 2012) consists of two circular plates each of inside radius b and outside radius a. The lower and upper plate rotates with angular velocities Ω_l and Ω_u respectively, about the z-axis. The upper disk moves towards the lower disk normally with uniform velocity $\dot{h_0}$. The bearing systems are assumed to be transversely rough.

The stochastically modeling of surface roughness by (Christensen & Tonder, 1969a,b, 1970) the thickness $h(x)$ is considered as

$$h(x) = \overline{h}(x) + h_s \tag{1}$$

where $\overline{h}(x)$ is the mean film thickness and h_s is the deviation from the mean film thickness characterizing the random roughness of the bearing surfaces.

h_s is assumed to be stochastic in nature and governed by the probability density function

$$f(h_s) = \begin{cases} \dfrac{35}{32c}\left(1 - \dfrac{h_s^2}{c^2}\right)^3 & , \; -c \leq h_s \leq c \\ 0 & , \; elsewhere \end{cases} \tag{2}$$

where c being the maximum deviation from the mean film thickness. The mean α, the standard deviation σ and the parameter ε, which is the measure of symmetry of the random variable are determined by the relationships

$$\alpha = E(h_s), \; \sigma^2 = E(h_s - \alpha)^2, \; \varepsilon = E(h_s - \alpha)^3 \tag{3}$$

where E denotes the expected value defined by

$$E(R) = \int_{-c}^{c} R \, f(h_s) \, dh_s \tag{4}$$

Axially symmetric flow of the magnetic fluid between the plates is taken into consideration under an oblique magnetic field

$$\overline{H} = \left(H(r)\cos\phi(r,z), 0, H(r)\sin\phi(r,z)\right) \tag{5}$$

whose magnitude H vanishes at $r = a$; for instance

$$H^2 = kr^2 \frac{(a-r)}{a}, \; 0 \leq r \leq a \tag{6}$$

where $k = 10^{14} \, A^2 m^{-4}$ chosen constant so as to have a magnetic field of required strength, which suits the dimensions. The direction of the magnetic field plays a significant role since $\overline{H}$ has to satisfy the relations

$$\nabla . \overline{H} = 0, \quad \nabla \times \overline{H} = 0 \tag{7}$$

Therefore, $\overline{H}$ arises out of a potential function and the inclination angle ϕ of the magnetic field $\overline{H}$ with the lower plate is determined by the following

$$\cot \phi \frac{\partial \phi}{\partial r} + \frac{\partial \phi}{\partial z} = \frac{1}{2(a-r)} \tag{8}$$

whose solution is determined from the equation

$$c_1^2 \cos ec^2 \phi = a - r, \quad z = -2c_1 \sqrt{a - c_1^2 - r} \tag{9}$$

where c_1 is a constant of integration.

The modified Reynolds equation governing the film pressure p under the usual assumptions of hydromagnetic lubrication takes the form (Abhangi & Deheri, 2012; Patel et al., 2009; Prajapati, 1992)

$$\frac{1}{r} \frac{d}{dr} \left[r \, g(h) \frac{d}{dr} \left(p - \frac{1}{2} \mu_0 \overline{\mu} H^2 \right) \right] = 12 \mu \dot{h}_0 + \rho \left(\frac{3}{10} \Omega_r^2 + \Omega_r \Omega_l + \Omega_l^2 \right) \frac{1}{r} \frac{d}{dr} \left[r^2 \, g(h) \right] \tag{10}$$

where

$$g(h) = h^3 + 3\alpha h^2 + 3(\alpha^2 + \sigma^2)h + 3\sigma^2\alpha + \alpha^3 + \varepsilon + 12\phi H_0, \quad \Omega_r = \Omega_u - \Omega_l \tag{11}$$

Introducing the non-dimensional quantities

$$\overline{h} = \frac{h}{h_0}, \; R = \frac{r}{a}, \; \mu^* = \frac{-\mu_0 \overline{\mu} \, k \, h_0^3}{\mu \dot{h}_0}, \; P = \frac{-h_0^3 p}{\mu a^2 \dot{h}_0}, \; \Omega_f = \frac{\Omega_l}{\Omega_u}, \; \overline{\sigma} = \frac{\sigma}{h_0}, \; \psi = \frac{\phi H_0}{h_0^3}$$

$$\overline{\varepsilon} = \frac{\varepsilon}{h_0^3}, \; \overline{\alpha} = \frac{\alpha}{h_0}, \; B = \beta a^2, \; C = \gamma a^2, \; S = \frac{-\rho \Omega_u^2 h_0^3}{\mu \dot{h}_0}, \; G(h) = \frac{g(h)}{h_0^3} \tag{12}$$

and solving the associated Reynolds equation with the concerned boundary conditions

$$P(1) = 0, \left(\frac{dP}{dR} \right)_{R=0} = -\frac{\mu^*}{2} \tag{13}$$

one gets the expression for nondimensional pressure distribution

$$P = \frac{1}{2} \mu^* R^2 (1-R) - \frac{3 \left(R^2 - 1 \right)}{G(h)} - \frac{S}{20} \left(3\Omega_f^2 + 4\Omega_f + 3 \right) \left(1 - R^2 \right) \tag{14}$$

where

$$G(h) = \frac{g(h)}{h_0^3} = \left(\frac{2+\overline{S}}{1+\overline{S}} \right) + 3\overline{\alpha} \left(\frac{2+\overline{S}}{1+\overline{S}} \right)^{2/3} + 3(\overline{\alpha}^2 + \overline{\sigma}^2) \left(\frac{2+\overline{S}}{1+\overline{S}} \right)^{1/3} + 3\overline{\sigma}^2 \overline{\alpha} + \overline{\alpha}^3 + \overline{\varepsilon} + 12\psi \tag{15}$$

The dimensionless load carrying capacity then, is given by the following

$$\overline{W} = \frac{-h_0^3}{2\pi \mu a^4 \dot{h}_0} w$$

$$\overline{W} = \frac{\mu^*}{40} + \frac{3}{4G(h)} - \frac{S}{80} \left(3\Omega_f^2 + 4\Omega_f + 3 \right) \tag{16}$$

where the load carrying capacity w is obtained from the relation

$$w = 2\pi \int_0^a r \, p \, dr \tag{17}$$

3. Results and Discussion

The graphical results presented here suggest the following.
1. The transverse roughness effect is in general adverse.
2. This adverse effect can be minimized to certain extend in the case of negatively skewed roughness by choosing a suitable magnetic strength and the rotation ratio. It is observed that the effect of skewness on the load with respect to rotation ratio remains nominal.
3. In fact in the above enhance performance the ratio of curvature parameter may also play a significant role.
4. It is noted that the effect of slip velocity on the variation of load carrying capacity with respect to

rotational inertia is almost negligible.

5. In addition, the variance negative adds to the positive effect of magnetic fluid lubrication.

4. Validation

Table 1. Comparison of Load carrying capacity calculated for μ^*

Quantity	Load carrying Capacity (calculated for $\alpha = 0.025, \sigma = 0, \varepsilon = 0.01, \psi = 0.01, S = -2, \Omega_f = -2, \overline{S} = 150, B = 0.01, C = 0.7$)	
μ^*	Result of the current study	(Abhangi and Deheri 2012)
0.01	0.793120	0.671685
0.02	0.793370	0.671935
0.03	0.793620	0.672185
0.04	0.793870	0.672435
0.05	0.794120	0.672685

Table 2. Comparison of Load carrying capacity calculated for α

Quantity	Load carrying Capacity (calculated for $\mu^* = 0.03, \sigma = 0.1, \varepsilon = 0.01, \psi = 0.01, S = -2, \Omega_f = -2, \overline{S} = 150, B = 0.01, C = 0.7$)	
α	Result of the current study	(Abhangi and Deheri 2012)
-0.05	0.909660	0.783170
-0.025	0.862270	0.729070
0	0.818600	0.693640
0.025	0.778320	0.661150
0.05	0.741150	0.631300

Table 3. Comparison of Load carrying capacity calculated for σ

Quantity	Load carrying Capacity (calculated for $\mu^* = 0.03, \alpha = -0.05, \varepsilon = 0.01, \psi = 0.01, S = -2, \Omega_f = -2, \overline{S} = 150, B = 0.01, C = 0.7$)	
σ	Result of the current study	(Abhangi and Deheri 2012)
0	0.930770	0.783170
0.05	0.925380	0.779240
0.1	0.909660	0.767780
0.15	0.884890	0.749600
0.2	0.852880	0.725960

Table 4. Comparison of Load carrying capacity calculated for ε

Quantity	Load carrying Capacity (calculated for $\mu^* = 0.03, \alpha = 0.025, \sigma = 0.1, \psi = 0.01, S = -2, \Omega_f = -2, \overline{S} = 150, B = 0.01, C = 0.7$)	
ε	Result of the current study	(Abhangi and Deheri 2012)
-0.02	0.793200	0.670760
-0.01	0.788160	0.667510
0	0.783200	0.664310
0.01	0.778320	0.661150
0.02	0.773520	0.658030

Table 5. Comparison of Load carrying capacity calculated for S

Quantity	Load carrying Capacity (calculated for $\mu^* = 0.03, \alpha = 0.025, \sigma = 0.1,\ \varepsilon = 0.01, \psi = 0.02, \Omega_f = -2, \overline{S} = 150, B = 0.01, C = 0.7$)	
S	Result of the current study	(Abhangi and Deheri 2012)
-4	0.900340	0.836150
-2	0.725340	0.661150
0	0.550340	0.486150
2	0.375340	0.311150
4	0.200340	0.136150

Table 6. Comparison of Load carrying capacity calculated for Ω_f

Quantity	Load carrying Capacity (calculated for $\mu^* = 0.03, \alpha = 0.025, \sigma = 0.1, \varepsilon = 0.01, \psi = 0.02, S = -2, \overline{S} = 150, B = 0.01, C = 0.7$)	
Ω_f	Result of the current study	(Abhangi and Deheri 2012)
-2	0.725340	0.661150
-1	0.600340	0.536150
-0.667	0.592000	0.527820
0	0.625340	0.561150
1	0.800340	0.736150

Table 7. Comparison of Load carrying capacity calculated for $\overline{S}$

Quantity	Load carrying Capacity (calculated for $\mu^* = 0.03, \alpha = 0.025, \sigma = 0.1,\ \varepsilon = 0.01, \psi = 0.02, S = -2, \Omega_f = -2$)	
$\overline{S}$	Result of the current study	(Abhangi and Deheri 2012)
50	0.719850	--
100	0.723940	--
150	0.725340	--
200	0.726040	--
250	0.726460	--

Table 8. Comparison of Load carrying capacity calculated for ψ

Quantity	Load carrying Capacity (calculated for $\mu^* = 0.03, \alpha = 0.025, \sigma = 0.1,\ \varepsilon = 0.01, S = -2, \Omega_f = -2, \overline{S} = 150$)	
ψ	Result of the current study	(Abhangi and Deheri 2012)
0.01	0.778320	--
0.015	0.750610	--
0.02	0.725340	--
0.025	0.702190	--
0.03	0.680910	--

Table 9. Comparison of Load carrying capacity calculated for various parameters

Quantity	Load carrying Capacity	
	Result of the current study	(Abhangi and Deheri 2012)
$\sigma = 0$	0.930770	0.783170
$\psi = 0.01$	0.778320	--
$S = -4$	0.900340	0.836150
$C = 0.9$	--	0.772480
$\overline{S} = 50$	0.719850	--

Lastly to validate our result, a comparison has been made with the investigations of (Abhangi & Deheri, 2012). It is seen that the results either compare well or there is a minor difference which may be due to the effect of slip. However, the curvature parameter of the upper plates goes ahead of the lower plate's curvature parameter, for improving the bearing performance.

5. Conclusion

This study concludes that surface roughness should be a primary concern with the designs of magnetic fluid based bearing system. The rotation and curvature parameters are to be selected carefully even if the slip is at the minimum level. The report also suggests that for a 'no flow' situation, the bearing can endure only a specific load amount. However, the study confirmed that the substantial impact of slip velocity and negatively skewed roughness can be streamlined to design bearing systems with more durability.

References

Hays, D. F. (1963), "Squeeze films for rectangular plates", *Journal of Basic Engineering* 85(2), 243–246.

Moore, D. F. (1965), "A review of squeeze films", *Wear* 8(4), 245-263.

Kuzma, D. C. (1968), "Fluid inertia effects in squeeze films", *Applied Scientific Research* 18(1), 15-20.

Christensen, H. & Tonder, K. C. (1969a), "Tribology of rough surfaces: stochastic models of hydrodynamic lubrication", *SINTEF Report 10/69-18*.

Christensen, H. & Tonder, K. C. (1969b), "Tribology of rough surfaces: parametric study and comparison of lubrication model", *SINTEF Report 22/69-18*.

Christensen, H. & Tonder, K. C. (1970), "The hydrodynamic lubrication of rough bearing surfaces of finite width", *ASME-ASLE Lubrication Conference*, 12-15.

Sparrow, E. M., Beavers, G. S. & Hwang, I. T. (1972), "Effect of velocity slip on porous walled squeeze films", *Journal of Lubrication Technology* 94(3), 260-264.

Wu, H. (1972), "An analysis of the squeeze film between porous rectangular plates", *Journal of Lubricant Technology* 94(1), 64-68.

Murti, P. R. K. (1973), "Squeeze films in porous circular disks", *Wear* 23(3), 283-289.

Prakash, J. & Vij, S. K. (1973), "Load capacity and time-height relations for squeeze films between porous plates", *Wear* 24(3), 309-322.

Gupta, J. L., Vora, K. H. & Bhat, M. V. (1982), "The effect of rotational inertia on the squeeze film load between porous annular curved plates", *Wear* 79(2), 235-240.

Prakash, J. & Tiwari, K. (1983), "Roughness effects in porous circular squeeze-plates with arbitrary wall thickness", *J. of Lubrication Tech.* 105(1), 90-95.

Prajapati, B. L. (1992), "Squeeze film behaviour between rotating porous circular plates with a concentric circular pocket: surface roughness and elastic deformation effects", *Wear* 152(2), 301-307.

Naduvinamani, N. B. & Gurubasavaraj, G. (2004), "Surface roughness effects on squeeze films in curved circular plates", *Industrial Lubrication and Tribology* 56(6), 346-352.

Kumar, J. V. & Rao, R. R. (2015), "Effects of surface roughness in squeeze film lubrication of two parallel plates", *Tribology in Industry* 37(2), 161-169.

Patel, K. C. (1980), "The hydromagnetic squeeze film between porous circular disks with velocity slip", *Wear* 58(2), 275-281.

Verma, P. D. S. (1986), "Magnetic fluid-based squeeze film", *International Journal of Engineering Science* 24(3), 395-401.

Shah, R. C. & Bhat, M. V. (2000), "Squeeze film based on magnetic fluid in curved porous rotating circular plates", *Journal of Magnetism and Magnetic Materials* 208(1), 115-119.

Tripathi, S. R., Bhat, M. V. & Shah, R. C. (2002), "Magnetic fluid based squeeze film between porous annular curved plates with the effect of rotational inertia", *Pramana* 58(3), 545-550.

Hsu, C. H., Lu, R. F., Lin, J. R. & Lai, C. (2009), "Combined effects of surface roughness and rotating inertia on the squeeze film characteristics of parallel circular disks", *Journal of Marine Science and Technology* 17(1), 60–66.

Patel, R. M. & Deheri, G. M. (2002), "Magnetic fluid based squeeze film between two curved plates lying along the surfaces determined by secant functions", *Indian journal of engineering and materials sciences* 9, 45-48.

Patel, H. C., Deheri, G. M. & Patel, R. M. (2009), "Magnetic fluid‑based squeeze film between porous rotating rough circular plates", *Industrial Lubrication and Tribology* 61(3), 140-145.

Patel, N. S., Vakharia, D. P., Deheri, G. M. & Patel, H. C. (2017), "Experimental performance analysis of ferrofluid based hydrodynamic journal bearing with different combination of materials", *Wear* 376-377, 1877-1884.

Shimpi, M. E. & Deheri, G. M. (2012), "Performance of magnetic fluid based squeeze film between a curved porous circular plate and a flat circular plate and effect of surface roughness", *Journal of the Serbian Society for Computational Mechanics* 6(2), 45-60.

Shimpi, M. E. & Deheri, G. M. (2012), "Magnetic fluid-based squeeze film behaviour in curved porous rotating rough annular plates and elastic deformation effect", *Advances in Tribology*, Article ID 148281.

Abhangi, N. D. & Deheri, G. M. (2012), "Numerical modeling of squeeze film performance between rotating transversely rough curved circular plates under the presence of a magnetic fluid lubricant", *ISRN Mechanical Engineering*, Article ID 873481.

Nomenclature

a	Radius of the upper plate
b	Radius of the lower plate
K	Aspect ratio b/a (width/height)
r	Radial coordinate
p	Pressure in the film region (N/mm^2)
B	Curvature parameter of the upper plate (m^{-1})
C	Curvature parameter of the lower plate (m^{-1})
H^2	Magnitude of Magnetic field (N/A.m)
P	Non-dimensional film pressure
w	Load capacity (N)
W	Non-dimensional load capacity
h_0	Central distance between the plates (mm)
$\dot{h_0}$	Normal velocity (m/s)
μ	Fluid viscosity (N.s/m^2)
μ_0	Permeability of the free space (N/A^2)
$\bar{\mu}$	Magnetic Susceptibility of particles
μ^*	Dimensionless magnetization parameter
α	Variance (mm)
ε	Skewness (mm^3)
ψ	Porosity
σ	Standard deviation (mm)
$\bar{\alpha}$	Non- dimensional Variance
$\bar{\varepsilon}$	Skewness in dimensionless form
$\bar{\sigma}$	Dimensionless standard deviation
$\bar{S}$	Slip parameter
S	Rotational inertia (kg/m^2)
Ω_f	Rotational speed (rad/s)
Ω_u	Angular velocity of the upper plate (rad/s)
Ω_l	Angular velocity of the lower plate (rad/s)
ρ	Fluid density (N.sec^2/m^4)
ϕ	Inclination angle ($^\circ$)
β, γ	Material constants
$\bar{H}$	External magnetic field
H_0	Thickness of porous facing
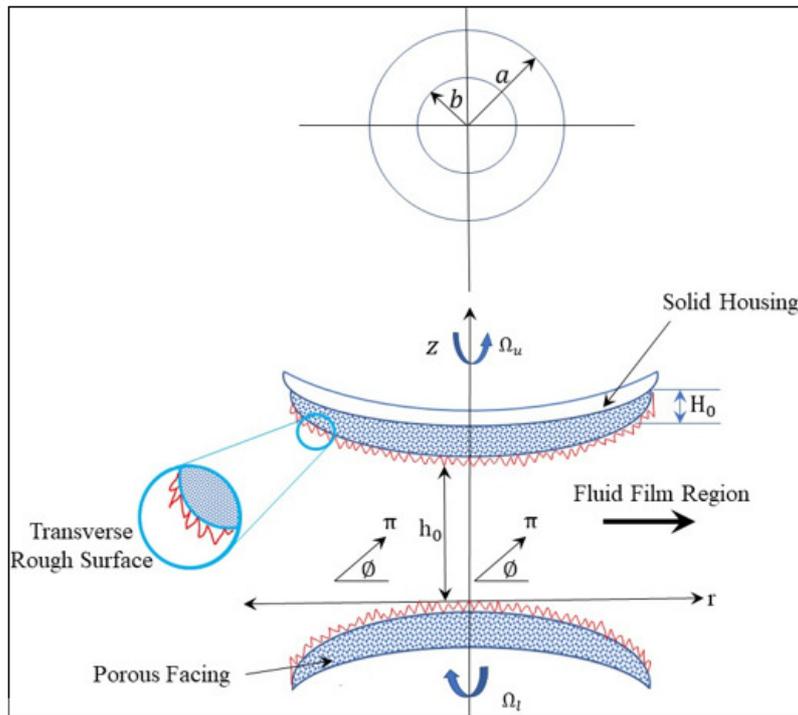
Figure 1. Configuration of bearing system
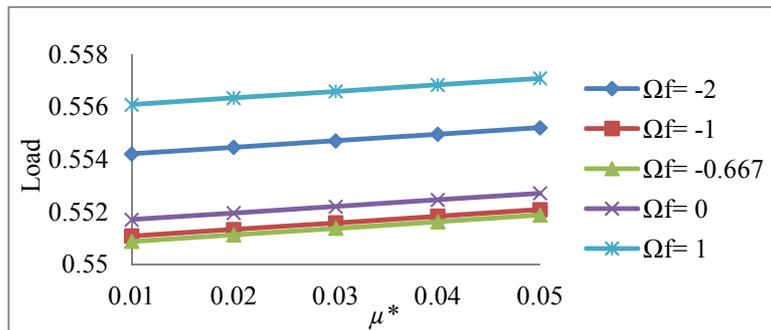
Figure 2. Variation of load carrying capacity with respect to μ^* and Ω_f
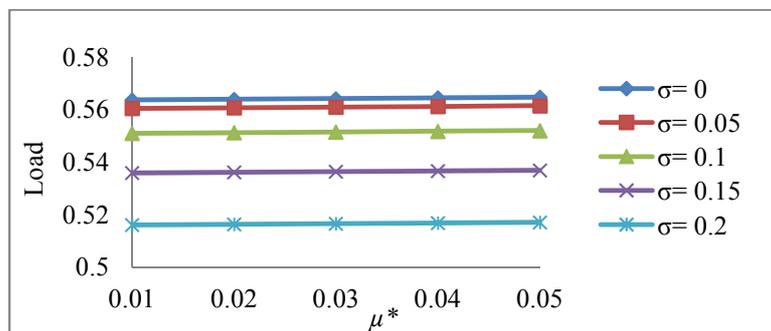
Figure 3. Variation of load carrying capacity with respect to μ^* and σ
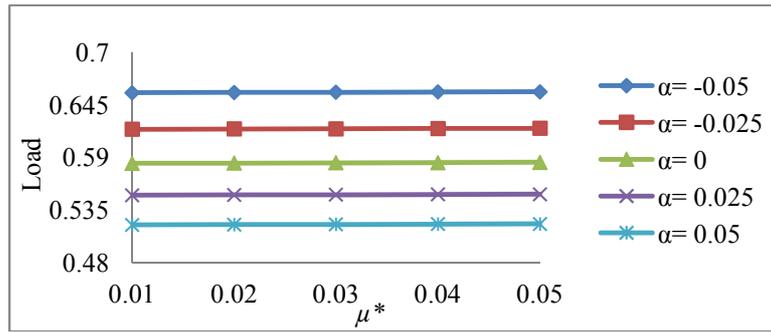
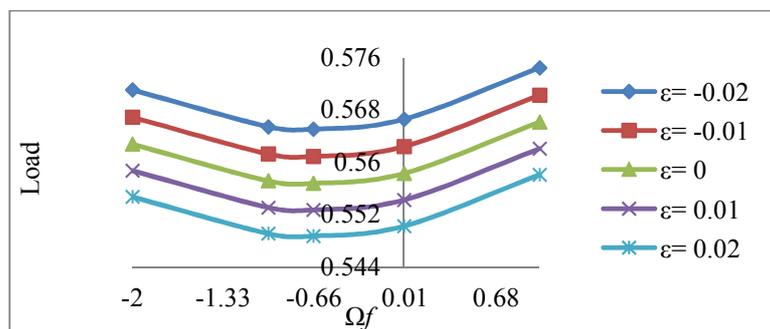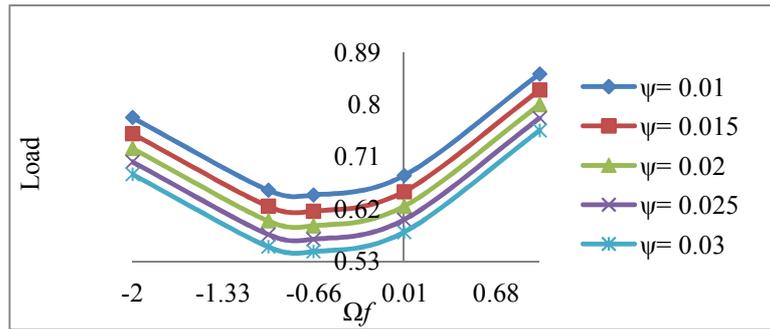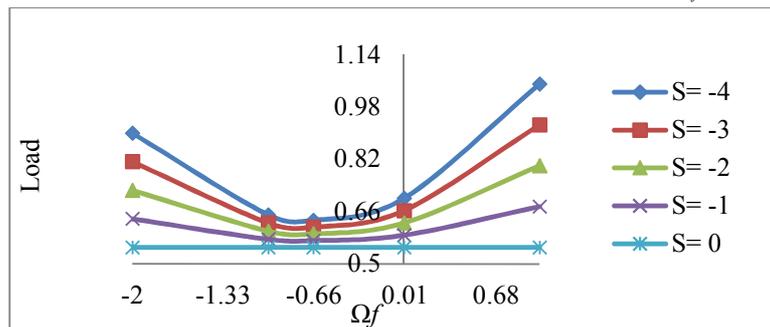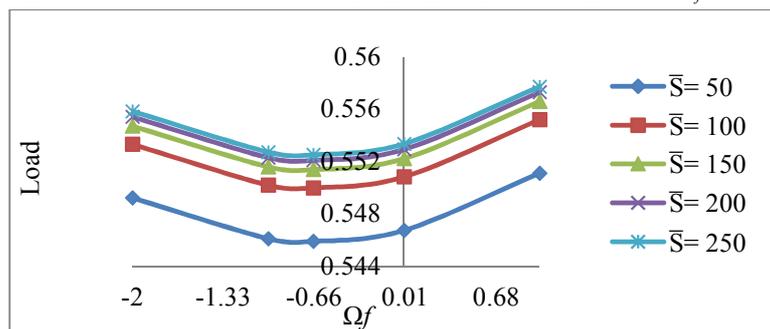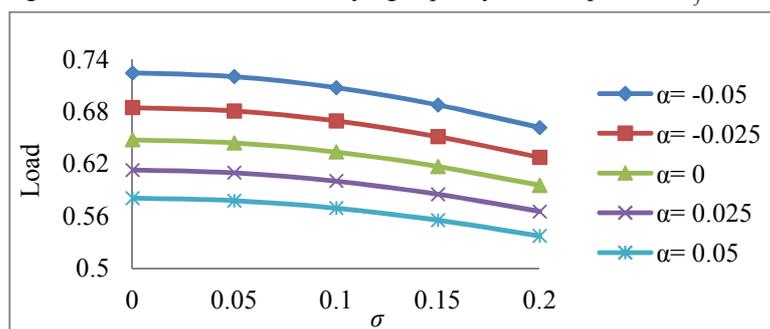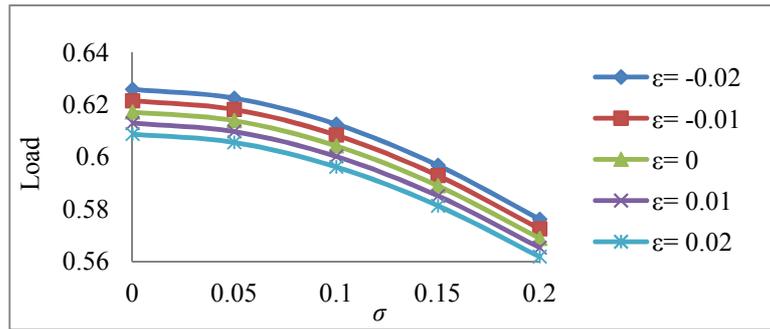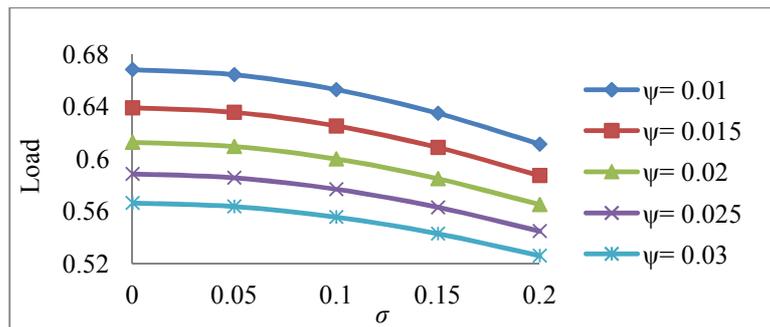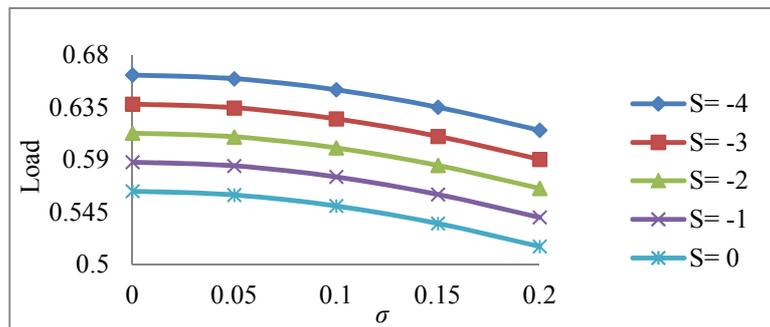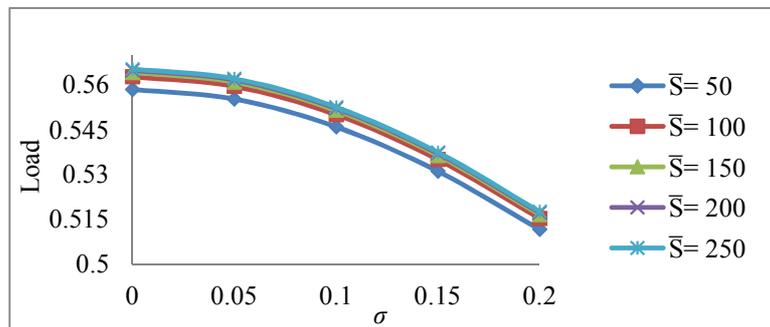Figure 4. Variation of load carrying capacity with respect to μ^* and α
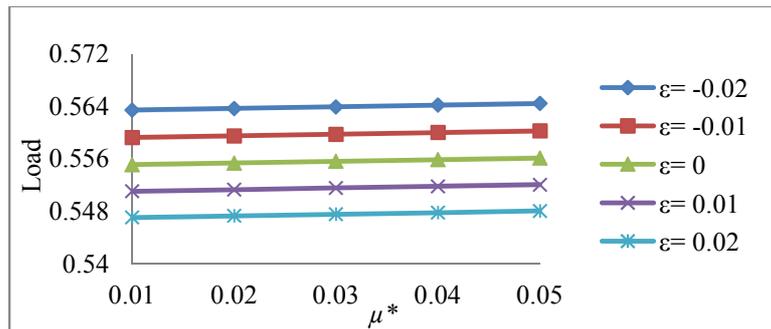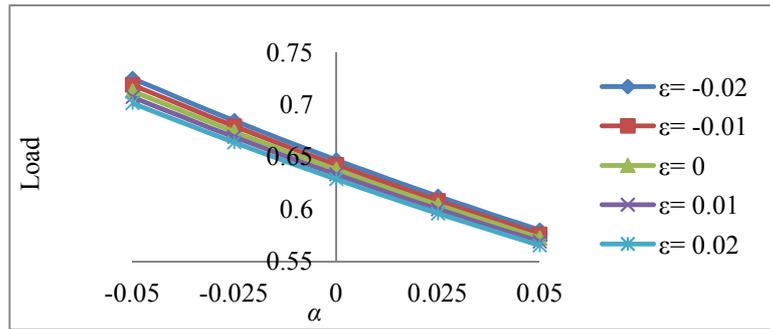

Figure 5. Variation of load carrying capacity with respect to μ^* and ε
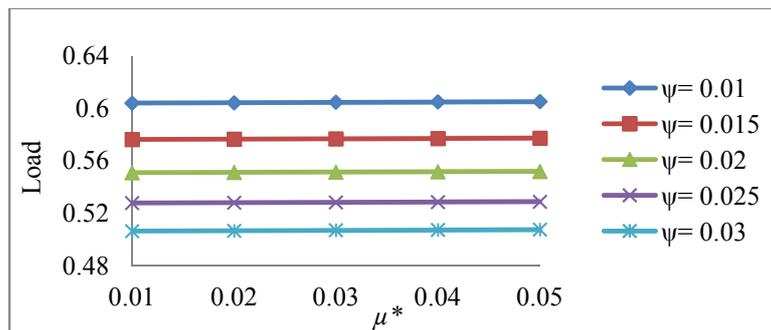
Figure 6. Variation of load carrying capacity with respect to μ^* and ψ
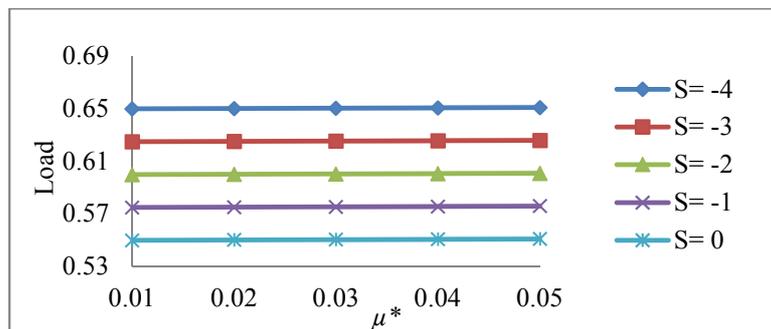
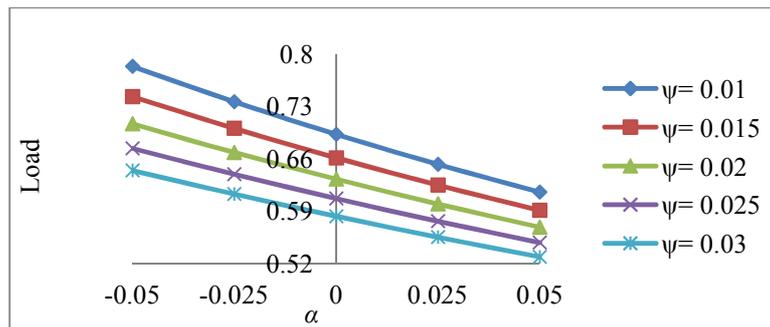Figure 7. Variation of load carrying capacity with respect to μ^* and S
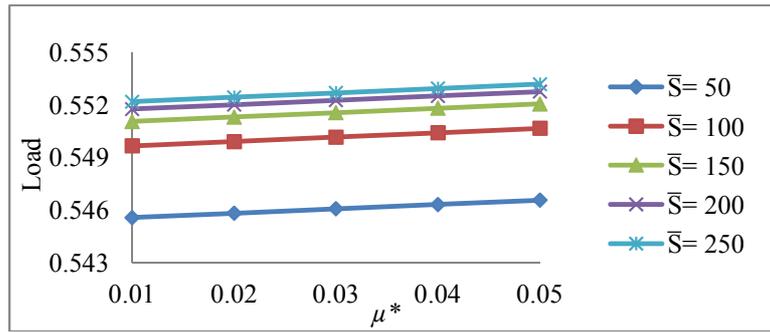
Figure 8. Variation of load carrying capacity with respect to μ^* and $\overline{S}$
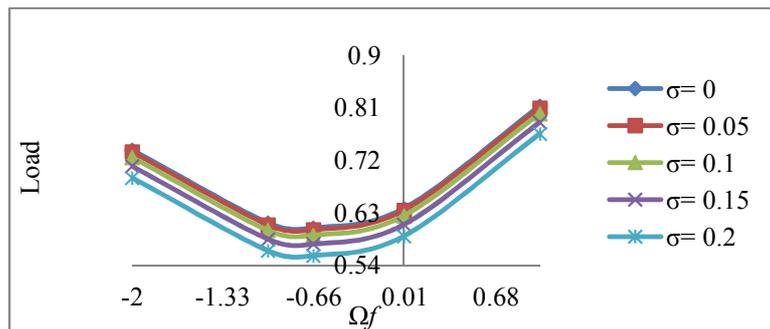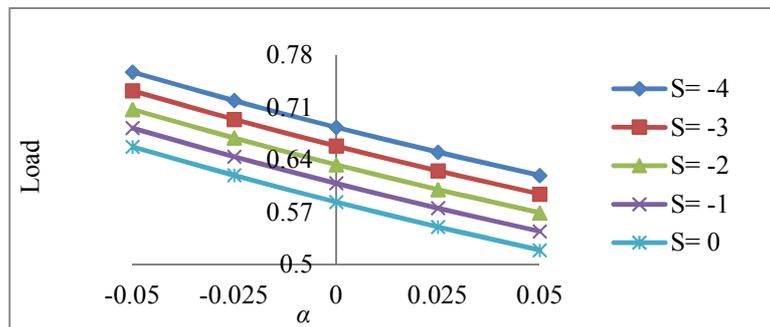

Figure 9. Variation of load carrying capacity with respect to Ω_f and σ
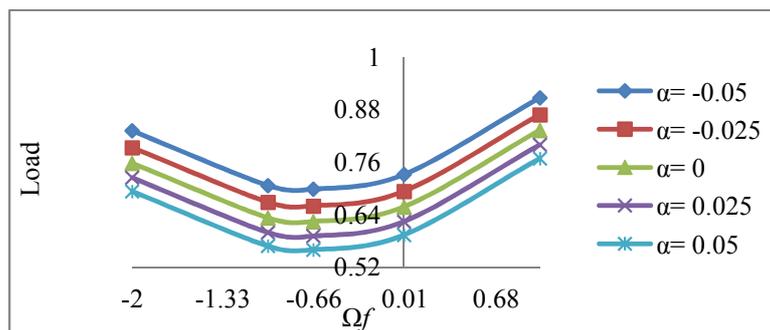
Figure 10. Variation of load carrying capacity with respect to Ω_f and α

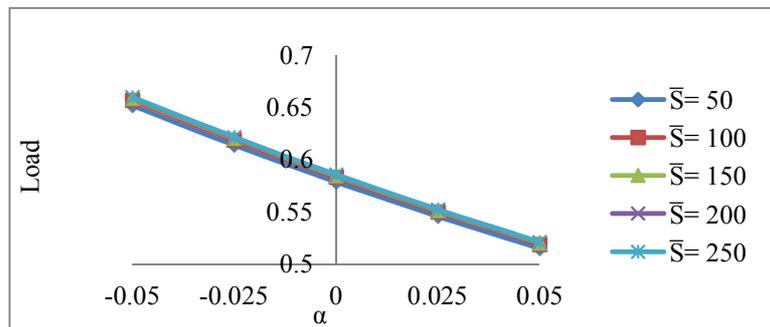Figure 11. Variation of load carrying capacity with respect to Ω_f and ε

Figure 12. Variation of load carrying capacity with respect to Ω_f and ψ

Figure 13. Variation of load carrying capacity with respect to Ω_f and S

Figure 14. Variation of load carrying capacity with respect to Ω_f and $\overline{S}$

Figure 15. Variation of load carrying capacity with respect to σ and α

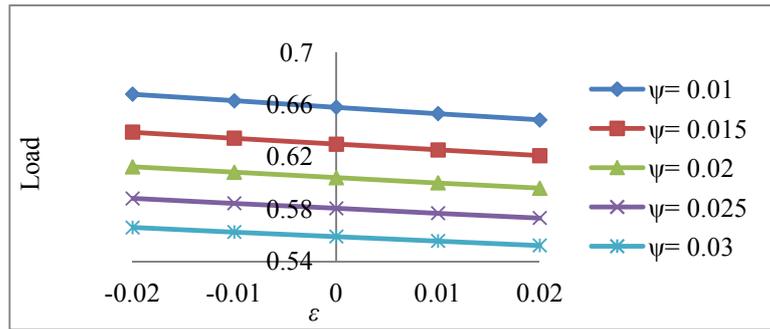Figure 16. Variation of load carrying capacity with respect to σ and ε
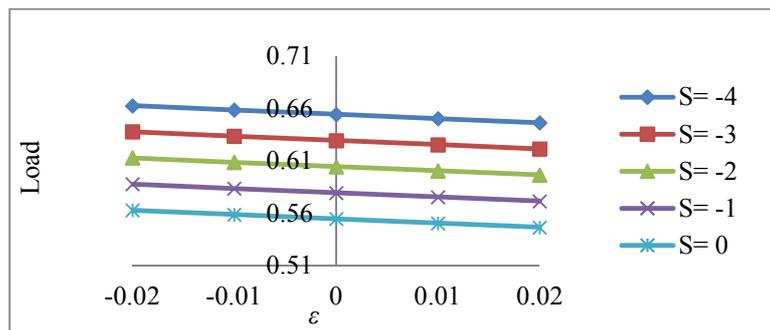

Figure 17. Variation of load carrying capacity with respect to σ and ψ

Figure 18. Variation of load carrying capacity with respect to σ and S

Figure 19. Variation of load carrying capacity with respect to σ and $\overline{S}$

Figure 20. Variation of load carrying capacity with respect to α and ε

Figure 21. Variation of load carrying capacity with respect to α and ψ

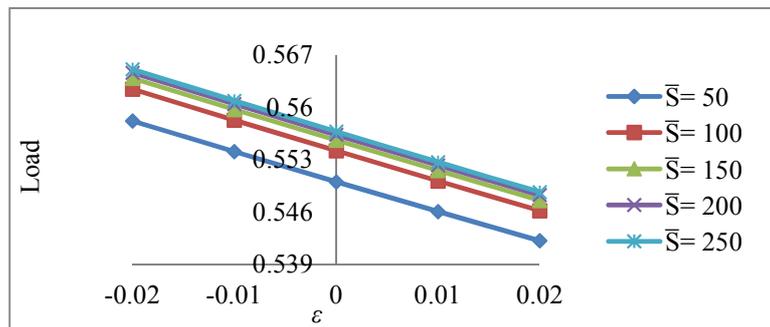Figure 22. Variation of load carrying capacity with respect to α and S

Figure 23. Variation of load carrying capacity with respect to α and $\overline{S}$

Figure 24. Variation of load carrying capacity with respect to ε and ψ

Figure 25. Variation of load carrying capacity with respect to ε and S

Figure 26. Variation of load carrying capacity with respect to ε and $\overline{S}$
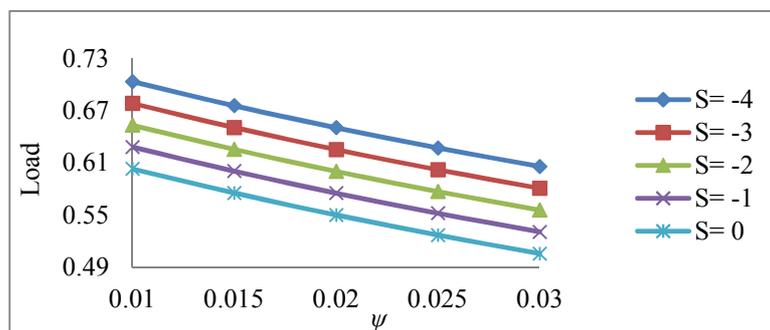

Figure 27. Variation of load carrying capacity with respect to ψ and S
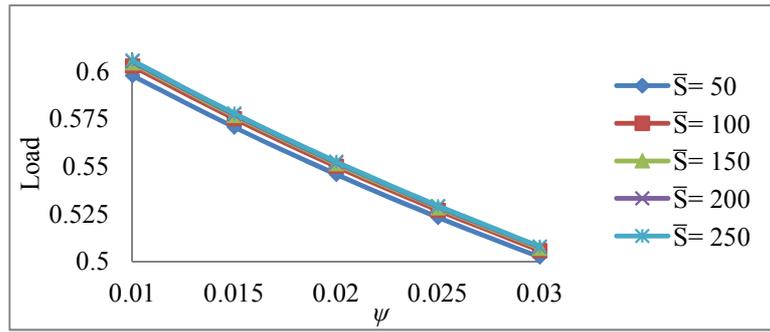
Figure 28. Variation of load carrying capacity with respect to ψ and $\overline{S}$
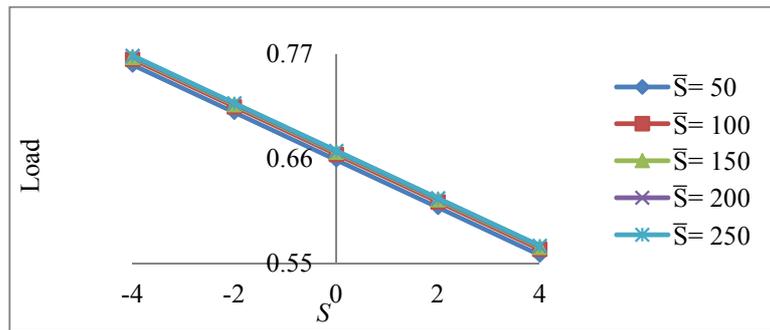

Figure 29. Variation of load carrying capacity with respect to S and $\overline{S}$